



Highly Dynamic Methane Emission from the West Siberian Boreal Floodplains

I. E. Terentieva¹ · A. F. Sabrekov^{1,2} · D. Ilyasov² · A. Ebrahimi³ · M. V. Glagolev^{1,2,4,5} · S. Maksyutov⁶

Received: 18 January 2017 / Accepted: 1 October 2018 / Published online: 25 October 2018
© Society of Wetland Scientists 2018

Abstract

The West Siberia Lowland (WSL) is one of the biggest wetland areas in high latitudes; however, measurements of gas fluxes from WSL floodplain wetlands were absent. During 2015–2016, we made first effort to estimate methane emission from floodplain using chamber method. Obtained fluxes varied greatly with medians from zero to $17.5 \text{ mgC}\cdot\text{m}^{-2}\cdot\text{h}^{-1}$. We found that observed heterogeneity could be addressed for further upscaling by grouping the flux observations using a set of environmental parameters: i) floodplain width (wide/narrow), ii) microtopography (elevated/depressed), iii) inundation during the measurements («wet»/«dry»). We found that several classes could be easily merged basing on CH_4 emission rates: i) flux median from both «wet» and «dry» depressions of wide floodplains reached $4.21 \text{ mgC}\cdot\text{m}^{-2}\cdot\text{h}^{-1}$, ii) «wet» elevations within wide floodplains and all small «wet» floodplains had lower flux of $1.47 \text{ mgC}\cdot\text{m}^{-2}\cdot\text{h}^{-1}$, iii) «dry» elevations within wide floodplains and all small «dry» floodplains had the lowest median of $0.07 \text{ mgC}\cdot\text{m}^{-2}\cdot\text{h}^{-1}$. Besides the common factors which influence the methane fluxes, we also found extreme methane emission during ten days after main water subsiding in Ob' floodplain with further gradual decreasing of fluxes and dispersions. We suggested that methane release could be triggered by abrupt hydrostatic pressure decrease induced by water drawdown.

Keywords Floodplain · Riparian wetlands · Greenhouse gases · Fluxes · Siberia · Taiga · Chamber method · Ebullition

Electronic supplementary material The online version of this article (<https://doi.org/10.1007/s13157-018-1088-4>) contains supplementary material, which is available to authorized users.

✉ I. E. Terentieva
kleptsova@gmail.com

M. V. Glagolev
m_glagolev@mail.ru

- ¹ Tomsk State University, 36 Lenina Street, Tomsk 643050, Russia
- ² Institute of Forest Science, Russian Academy of Sciences, 21 Sovetskaya st., Uspenskoe, Moscow region 143030, Russia
- ³ Department of Environmental Systems Science, ETH Zurich, 8092 Zurich, Switzerland
- ⁴ Yugra State University, 16 Chekhova st., Khanty-Mansyisk 628012, Russia
- ⁵ Moscow State University, 1 Leninskie gory, Moscow 119992, Russia
- ⁶ National Institute for Environmental Studies, 16-2 Onogawa, Tsukuba, Ibaraki 305-8506, Japan

Introduction

Riparian wetlands are unique environments due to their spatial distribution in landscapes that are ecotones between the terrestrial and aquatic zones and corridors across regions (Malanson 1993). The soil biogeochemistry in riparian wetlands regularly changes by seasonal flooding and drying cycles. Particularly, methane production from riparian wetlands by methanogenic archaea may cause significant CH_4 emissions to the atmosphere (Stocker et al. 2013). In general, wetlands are considered as the largest natural source of methane emission which contributes for approximately 25% of the annual methane fluxes to the atmosphere (Whalen 2005; Nahlik and Mitsch 2010). Favorable environmental conditions in riparian wetlands including, anoxic conditions and soil with rich organic matter are optimal for methanogenic activity (Bartlett and Harriss 1993; Segers 1998). Despite the theoretical understanding that highlights the role of floodplains in methane emission, modern estimates of riverine

gas fluxes include only the main river channel in contrast to the theoretical framework concerning the role of floodplains which is less developed (Cole et al. 2007). Much of the uncertainty arises from the lack of field data, especially in the remote regions. For instance, seasonal floodplains of many high-latitude rivers are almost not presented in studies on methane emission. The only large-scale estimations of methane fluxes for the floodplains are conducted for the Amazon region (Melack et al. 2004; Ringeval et al. 2014).

Basin-wide estimate of annual methane emission is complicated due to potential seasonality of methane emissions caused by flow pulses and uncertainties in the areal extent and variability of methane-producing environments. Seasonal fluctuations in the water table level (WTL) may provoke ebullition due to hydrostatic pressure drops (Schütz et al. 1989; Sharkey et al. 1991; Tokida et al. 2007). This leads to high temporal heterogeneity intensified by mosaic structure of sediments and vegetation. According to Pulliam (1993) about 30% of floodplain that was continuously inundated accounts for more than 90% of the total floodplain CH₄ emissions.

West Siberian Lowland (WSL) is one of the most paludified region in the world experiencing accelerated rate of climate change (Stocker et al. 2013). Ob' is the westernmost of the three great Siberian rivers that flow into the Arctic Ocean and has a basin of about 2.97×10^6 km². Despite its great importance, field observations of the methane fluxes in Ob's domain were mainly focused on peatlands (Glagolev et al. 2011; Kim et al. 2011; Bohn et al. 2015) and lakes (Repo et al. 2007) with no field measurements concerning floodplain area to our knowledge.

The only available data comes from series of aircraft measurements of CH₄ concentration and turbulent parameters made in 1993 over the middle taiga zone (Postnov et al. 1994). These data show that the methane flux under Ob', Irtysh and Konda Rivers was high and exceeded this over treeless wetlands for an order of magnitude. Smaller rivers tended to produce the same effect but not so pronounced. However, the specified uncertainty of the calculated fluxes decreases its applicability.

The present study was motivated by the need for a systematic evaluation of temporal and spatial dynamics of methane fluxes from West Siberian floodplains under highly fluctuating water table levels. The specific objectives were: i) to measure and analyze methane emission rates using static chamber method from West Siberian floodplains; ii) to classify floodplains based on their characteristic elements for further upscaling of methane fluxes, iii) to evaluate the contribution of different methane transport mechanisms from WSL floodplains (e.g., diffusion and bubble ebullition).

Materials and Methods

Methods

Flux measurements were made by using static chambers ($30 \times 30 \times 40$ cm³) as it was described in (Sabrekov et al. 2014). Methane concentrations were measured by a gas chromatograph 'Crystall-5000' ('Chromatec' Co., Ioshkar-Ola, Russia) with an FID and column (3 m) filled by HayeSep Q (80–100 mesh) at 70 °C with nitrogen as a carrier gas (flow rate 30 ml min⁻¹) or by a modified gas chromatograph HPM-4 ('Chromatograph', Moscow, Russia) having a flame ionization detector of a chromatograph LHM-80 ('Chromatograph', Moscow, Russia), 1 m stainless steel column (2.5 mm o.d.) filled with Sovpol (80–100 mesh), at 40 °C with hydrogen as a carrier gas (flow rate 5 ml/min). The loop volume was 0.5 ml and the volume of injected sample was 3–4 ml. Each gas sample from a syringe was analyzed three times; the mean of the three concentrations was used for the flux calculation. The gas chromatograph was calibrated with standard gases (1.99 ± 0.01 , 5.00 ± 0.01 and 9.84 ± 0.01 ppmv methane in a synthetic air) prepared at the National Institute for Environmental Studies, Japan. The R² values for the linear correlation between signal (area of peak) and concentration in the standard were 0.998 and higher. The error of concentration measurement (standard deviation as percent of the mean of 6 to 10 daily repetitions of the standard) was typically 0.5% for the 1.99 ppmv CH₄ standard. Units were converted from ppmv to mgCH₄ m⁻³ using the ideal gas law. Methane fluxes were calculated from linear regression with the weights (Kahaner et al. 1989) for the chamber headspace CH₄ concentration versus measuring time.

At each site, the following environmental factors were measured: water table level (negative values mean that water stands above the surface), air and peat temperatures (at depths of 0, 5, 15, 45 cm; in 2016 all substrate temperatures were measured in water because of the flooding) by temperature loggers 'TERMOCHRON' iButton DS 1921–2 (DALLAS Semiconductor, USA), pH and electroconductivity by Combo 'Hanna 98129' ('Hanna Instruments', USA). Botanical descriptions were also made.

Surface water was sampled to analyze dissolved CH₄ concentrations, during the chamber measurements. Water samples were taken from a depth of 10 cm, then with intervals of 0.5 m and from bottom waters (maximum depth was 2.5 m). Plastic bottles of 50 and 100 ml were used for water storage; their full volume was filled with water. To reduce methane oxidation, samples were kept in refrigerator. Then, water samples of 20 ml volume were taken in the syringe and shaken vigorously for 2 min with 20 ml headspace with known atmospheric CH₄ concentration. CH₄ concentrations in headspace gas were analyzed in two replications in a field laboratory on a gas chromatograph as described above during the day after water

sampling. Dissolved CH_4 concentrations in water samples were calculated with Henry's law taking into account the temperature dependence of solubility (Krasnov et al. 2015). Simple gradient approach where difference between the actual CH_4 concentration in the surface water and CH_4 concentration in surface water in equilibrium with the atmosphere is multiplied on empirical exchange coefficient were used to calculate diffusional fluxes according to Rasilo et al. (2015). The atmospheric concentrations used in the calculations were the concentrations of CH_4 in ambient air, sampled with polypropylene syringes at 1 m above the water surface during the chamber measurements. For statistical analysis STATISTICA 12.5 (Dell Software, United States) was used.

Objects

First test site was located at the Ob' River floodplain near Khanty-Mansiysk city, Russia (Fig. 1; 61.08977°N, 69.45513°E). Ob' River is a major river in West Siberia and one of the longest rivers in the world. Due to the flat relief of WSL, it has slow stream velocity and wide floodplain with the river splitting into more than one arm. Water level usually reaches minimum values in August until October; however, rarely floodplain remained inundated until the middle of the August, as it had been observed during 2015 summer period.

In 2015, measurement sites were situated at the Ob' River floodplain at the distance up to 100 m from forest edge. Water levels were 20–40 cm above the soil surface at the beginning of measurements. During four days (from August 13 to 17) the water level dramatically dropped and the soil surface exposed to the air. It was still water saturated and in some areas water level still reached 5 cm above the soil surface. Further, soil gradually dried up and areas of saturated soil constantly decreased. Spatial variability of the fluxes within local depressions were represented by sites Ob.dep.1–3; local elevations were represented by sites Ob.el.wet.1 and Ob.el.dry. Temporal variability of fluxes were represented by two pairs of

measurement sites (Ob.ts.1–2 and Ob.ts.3–4; “ts” – means “time series”, see Table 1 and Fig. 3) located at the distance of 5 m from each other at the local depression. Within the pairs, chambers were located at the distance of 1 m; measurements within the pairs were carried out simultaneously.

In 2016, measurements within the Ob' floodplain were made at three sites: i) Ob.dep.4 represented local depression within the small inundated channel covered by sedge vegetation and corresponded to the previously measured Ob.dep.1–3 sites; ii) Ob.dep.5 represented the center of expanse depression with water level about –250 cm (negative values means that water is above the surface) without vegetation; iii) Ob.el.wet.2 represented elevated area of floodplain during the flooding period with water level of –70 cm and sedge vegetation.

In addition, several measurements were made within relatively narrow floodplains (up to 1 km of width). Test sites Mu.wet.1–2 were located at the Mukhrino creek, a small tributary of Ob' river, which has a length of 10 km and a maximal width of about 100–200 m. The river course has a size of several meters when the water is low; after snowmelt all floodplain is inundated with water level up to 2 m. Test sites were located at 1 km from the riverhead of the nearby peatland. All measurements were made in June 2016 when water was high after snowmelt.

Measurements were also carried out in two narrow floodplains in Tomsk region, Russia in August 2015. Test site Sheg.dry was located at Shegarka River floodplain (56.74137°N, 82.57743°E), at 15–30 m distance from the main channel. Vegetation consisted of willow and sparse shade-enduring plants. Test sites Bakch.wet.1 (in local depression) and Bakch.dry (in local elevation) represented the floodplain of Bakchar River tributary (56.95328°N, 82.50813°E). Vegetation consisted of different sedges with the high projective cover. Bakch.wet.1 site experience prolonged inundation during the growing season (WTL was from –20 to –10 cm); test site Bakch.dry was not flooded (WTL was 40 cm).

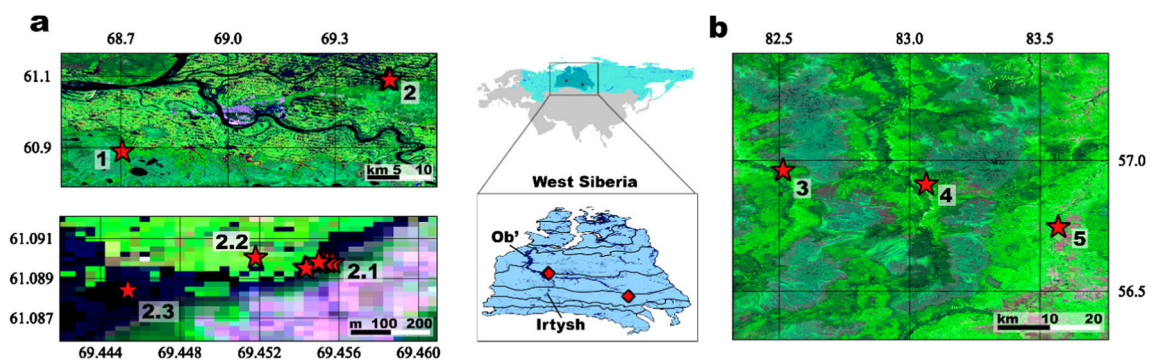


Fig. 1 Test sites in middle (a) and south (b) taiga zone: 1 – Mukhrino floodplain («Mu.wet»), 2 – Ob' floodplain (2.1 – «Ob.dep.1–4», «Ob.ts.1–4», «Ob.el.wet.1», «Ob.el.dry»); 2.2 – «Ob.el.wet.2»; 2.3 – «Ob.dep.5»), 3 – Bakchar floodplain («Bakch»), 4 – Yarya floodplain («Yarya»), 5 – Shegarka floodplain («Sheg»). Pink color represent

forests, dark blue – inundated floodplain depressed area, and light green – non-inundated floodplain elevated area at the Fig. 1a. Ob.dep.1–5 sites are located at the same depression; Ob.dep.1–4 represents its edge and Ob.dep.5 – the central area

In July–August 2016, WTL in Bakchar River tributary was significantly higher than in 2015. Measurements were carried out on test sites Bakch.wet.2 (WTL was from -15 to -40) and Bakch.wet.3 (WTL was from 10 to -40) that situated in local depression and local elevation respectively. Test sites Yarya.wet and Yarya.dry was located at Iksa river floodplain (56.90845°E , 83.06378°E , Tomsk region, Russia) at 1 – 5 m distance from the main channel and were characterized by intermittent inundation during the growing season. Yarya.wet site was located in local depression and Yarya.dry site – in local elevation.

Results

Spatial Variability of Methane Fluxes

Methane emissions from West Siberian floodplains are shown in Table 1. Flux medians varied in two orders of magnitude, from zero emissions at the driest environments to $17.5 \text{ mgC}\cdot\text{m}^{-2}\cdot\text{h}^{-1}$ at the local depression within Ob' floodplain. Observed variability complicates basin-wide estimate of annual methane emission due to unknown areal extent of ecosystems with different flux rates. To manage such heterogeneity, we aimed at developing classification of floodplain structural elements based on their abundance and ecological roles. Such a classification facilitates not only upscaling of methane fluxes to the regional scale but also guides further field investigations in this region.

As a first step, the studied floodplains were grouped into wide (about 20 – 30 km in our case) and narrow ones (about tens and first hundreds of meters width). The floodplain width may be used for generic prediction of hydrological regime, geochemical conditions, and sediment type. There are only a few large rivers in West Siberia but they occupy vast areas and can be more important at the regional scale compared to the smaller ones. As a second step, wide floodplains were considered as a combination of elevated and depressed areas. Depressed parts are characterized by hygrophilous vegetation and higher silt content in sediments. They experience prolonged inundation and the water level may reach several meters above the surface during the flood events. After water subsiding, soil may remain water saturated for a long period of time. Elevated parts are inundated for a shorter time period; afterwards the soil rapidly dries out due to the better drainage and sandy sediments. Depressed and elevated parts may form single flooded area during the flood. Unfortunately, these structural elements cannot be clearly defined within narrow floodplains. As a last step, measurement conditions were divided into «wet» (WTL < 0) or «dry» (WTL > 0) depending on the inundation level during each individual measurement. In contrast to previous steps, «wet» and «dry» conditions

correspond to the temporal variability more than spatial ones; they also highlight water level effect on methane fluxes.

This scheme including six types of environments was chosen to represent all variety of West Siberian floodplain landscapes. However, when measured fluxes were distributed among them, several classes were found to be similar in CH_4 emission rates: i) depressed «wet» and «dry» areas within wide floodplains, ii) «dry» areas within narrow floodplains and «dry» elevations within wide floodplains, iii) «wet» areas within narrow floodplains and «wet» elevations within wide floodplains. Therefore, these ecosystems were merged; final classes and their methane emission rates are represented in Table 2. The probability distribution functions of flux measurements from each ecosystem type are shown in Fig. 2. This observation highlights considerably high spatial variability of methane emission especially from depressions within wide floodplains, where a few rare but large emission events can contribute significantly to the total emission rates.

The results of this analysis show that methane fluxes from depressions within wide floodplains were highest reaching to $4.21 \text{ mgC}\cdot\text{m}^{-2}\cdot\text{h}^{-1}$ with interquartile range¹ (IQR) of $5.17 \text{ mgC}\cdot\text{m}^{-2}\cdot\text{h}^{-1}$. However, emission rates were weakly connected to the water table level; in particular, there were only slight difference between fluxes observed within «wet» and «dry» depressions. It can be explained by the presence of constant overwetting due to close position of underground waters or water accumulation after precipitation periods. The results also indicate that within elevations, inundated («wet») areas had higher CH_4 emission median of $1.47 \text{ mgC}\cdot\text{m}^{-2}\cdot\text{h}^{-1}$ with IQR of $2.99 \text{ mgC}\cdot\text{m}^{-2}\cdot\text{h}^{-1}$, compared to not inundated («dry») – $0.07 \text{ mgC}\cdot\text{m}^{-2}\cdot\text{h}^{-1}$ with IQR of $0.26 \text{ mgC}\cdot\text{m}^{-2}\cdot\text{h}^{-1}$.

To verify the statistical reliability of the separation ecosystems into three groups, we used the ANOVA to test differences in logarithmically transformed fluxes (initially distributed lognormally) between categories of ecosystems (Table 2). The normality of the distribution was confirmed using the Kolmogorov-Smirnov test. Since N were different in categories, Tukey HSD for unequal N test was used. The level of significance ($P < 0.05$) in pairs 1–2 (wide floodplains, «wet» and «dry» depressions – wide floodplains, «dry» elevations and small «dry» floodplains), 1–3 (wide floodplains, «wet» and «dry» depressions – wide floodplains, «wet» elevations and small «wet» floodplains) and 2–3 was 0.00022 , 0.000024 and 0.00022 respectively.

Temporal Variability of Methane Fluxes

Time-series measurements started at Ob.ts.1–4 sites when water table level was about the soil surface, just after main water subsiding. Figure 3 shows changes in emission rates during the measurement period and its relation to the water table

¹ Simple difference between third and first quartiles

Table 1 Methane flux medians and corresponding environmental conditions for West Siberian floodplains (negative WTL means that water stands above the surface)

Site	Date	Median, mgC·m ⁻² ·h ⁻¹	IQR, mgC·m ⁻² ·h ⁻¹	WTL _{mean} , cm	N ^a	Temperature, °C		
						T _{air}	T _{5cm}	T _{45cm}
Wide river floodplain (Ob' river)								
Ob.dep.1	12.08.15	7.3	2.5	-33	4	18.2	18.2	16.7
Ob.dep.2	13.08.15	6.8	3.2	-34	6	20.4	20.3	16.2
Ob.dep.3	17.08.15	6.3	1.7	-1	4	18.4	15.3	14.9
Ob.dep.4	20.06.16	1.0 / 0.27 ^b	1.0 / 0.01 ^b	-62	5	24.8	22.8	21.8
Ob.dep.5	20.06.16	3.8 / 0.12 ^b	1.9 / 0.05 ^b	-250	6	24.8	22.8	21.8
Ob.ts.1	17–28.08.15	1.2	2.3	1	10	11.5	12.1	12.0
Ob.ts.2		5.0	16.9	-2	10	11.5	12.1	12.0
Ob.ts.3	19–28.08.15	6.4	14.9	-3	6	11.9	11.0	10.9
Ob.ts.4		17.5	20.2	-1	6	11.9	11.0	10.9
Ob.el.wet.1	12.08.15	0.7	1.4	-21	6	18.1	18.6	16.6
Ob.el.wet.2	20.06.16	1.2	1.9	-70	4	24.8	22.8	21.8
Ob.el.dry	28.08.15	0.3	0.0	100	2	11.6	9.4	
Narrow river floodplains								
Sheg.dry	07.08.15	0.0	0.0	100	15	15.1	16.2	15.7
Bakch.wet.1	14.08.15	1.8	2.0	-15	10	19.0	17.6	14.0
Bakch.dry	14.08.15	0.1	0.1	40	3	19.0	15.5	13.5
Bakch.wet.2	21.07–7.08.16	8.9	6.4	-11	27	25.0	17.1	14.3
Bakch.wet.3		0.9	0.9	-27	20	28.2	17.0	13.8
Yarya.dry	22.7.16	0.5	0.5	25	8	21.6	18.7	14.4
Yarya.wet		6.2	6.8	-13	8	21.7	19.6	14.5
Mu.wet.1	19.06.16	0.4 / 0.13 ^b	0.2 / 0.06 ^b	-150	6	26.4	23.2	28.8
Mu.wet.2	19.06.16	0.9	0.4	-100	6	26.4	23.5	22.4

^a Number of measurement replications; ^b Diffusive CH₄ flux and its uncertainty

level. Water table level was calculated as a mean value across all sites that were measured on a certain day (e.g. WTL 17.08.2016 is a mean value across Ob.ts.1 and Ob.Ts.2). First, we found sudden peak in emissions just after the main water subsiding (13–17 of August) comparing to the flooding period. Second, results indicated a drop of CH₄ fluxes and their dispersions to the end of the measurement period:

median was 5.89 mgC·m⁻²·h⁻¹ for 14–24 of August and 3.51 mgC·m⁻²·h⁻¹ for 28 of August. Only Ob.ts.1 showed no clear dynamic (and low fluxes), maybe due to some local features of sediments.

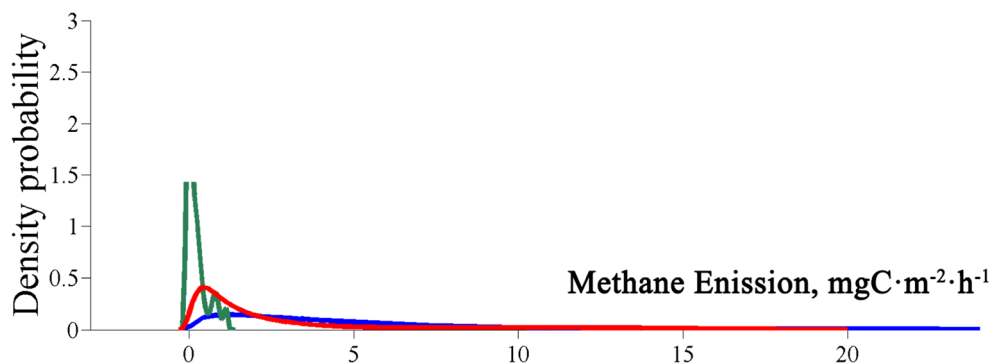
The temporal heterogeneity of fluxes among replications at individual sites was extremely high due to the active ebullition. However, the averaged fluxes of the replicates resulted in

Table 2 Spatial variability of methane fluxes from West Siberian floodplains

	Ecosystem type	Median, mgC·m ⁻² ·h ⁻¹	IQR, mgC·m ⁻² ·h ⁻¹	N ^a	Sites
1	Wide floodplains, «wet» and «dry» depressions	4.21	5.17	61	Ob.dep, Ob.ts
2	Wide floodplains, «dry» elevations and small «dry» floodplains	0.07	0.26	30	Ob.el.dry Bakch.dry, Sheg.dry, Yarya.dry
3	Wide floodplains, «wet» elevations and small «wet» floodplains	1.47	2.99	87	Ob.el.wet, Bakch.wet, Mu.wet, Yarya.wet

^a Number of measurements

Fig. 2 Probability density functions of methane fluxes: blue – «wet» and «dry» depressions of wide floodplains, green – «dry» elevations of wide floodplains combined with small «dry» floodplains, red – «wet» elevations of wide floodplains combined with small «wet» floodplains



more consistent emission dynamic patterns. In particular, the differences in their rates remained relatively constant during the measurement period with emission sequentially: Ob.ts.4 > Ob.ts.3 > Ob.ts.2 > Ob.ts.1 (Fig. 3).

Dissolved Methane Concentrations

Diffusive methane fluxes were calculated for three sites using concentration data (Fig. 4) and ranged from 0.12 to 0.27 mgC·m⁻²·h⁻¹ (Table 1). The total methane flux was measured by static chamber, i.e. it included diffusion as well as ebullition and plant-mediated transport. The highest total methane flux and the lowest diffusive emission rate were found at the Ob.dep.5 site. Contribution of diffusive flux to the total emission was only 3% while 97% of the flux should be considered as ebullition since there were no vegetation at the Ob.dep.5 site. Oppositely, diffusive flux accounted for 30% at Mu.wet.1 and Ob.dep.4 sites. At the same time, dissolved methane concentrations in bottom waters (10 cm above the sediments) was substantially lower at Mu.wet.1 and Ob.dep.4 (11.1 and 7.9 mgC/m³, respectively) in comparison to Ob.dep.5 (98.1 mgC/m³). Methane concentration in bottom waters was more than 10 times higher comparing to the surface layer at both

Ob.dep.4 and Ob.dep.5 sites; at the Mukhrino floodplain, it was only 3 times higher.

Discussions

Comparison with Literature Data

Due to the lack of literature data, the direct comparison of the fluxes obtained for the same climatic conditions is limited and similar ecosystems are considered for the sake of comparison. Concerning geographically the same area, overall flux range well agrees with emission rates from nearby peatlands (–0.08 to 58 mgC·m⁻²·h⁻¹; Sabrekov et al. 2011). Also, obtained fluxes are generally within the range reported for other riverine wetlands all over the world (Table 3). Emission from floodplains can reach the same level as in peatlands because in floodplains anaerobic degradation of organic matter necessary for methane production also occurs. Organic matter comes from floodplain vegetation with addition from river water during flooding (van Huissteden et al. 2005). Anaerobic conditions are determined by high ground water level (which is typical near terrace edge) and water income during the flood. Floodplain sediments near terrace edge often

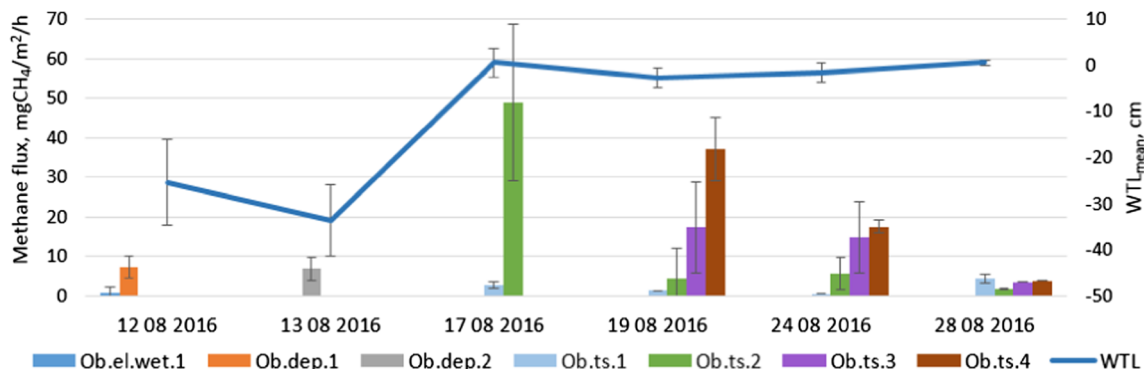
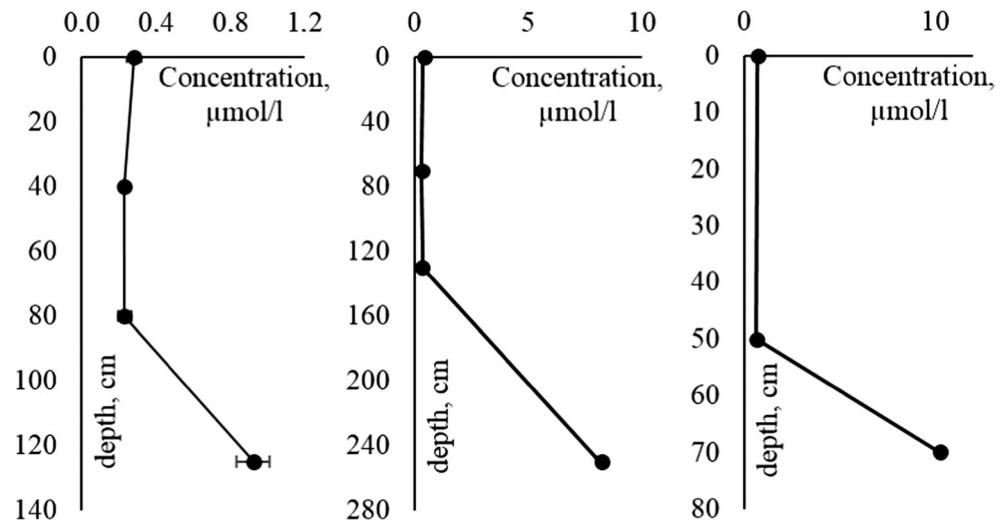


Fig. 3 Changes in emission rates during the measurement period and its relation to the WTL in August 2015. WTL is a daily mean value across the measured sites. Sudden peak in emissions was found after the main

water subsiding (13–17 of August) comparing to the flooding period (before August 13). We also indicated a drop of CH₄ flux magnitudes and their dispersions at the end of the measurement period

Fig. 4 Dissolved methane concentrations profiles for Mu.wet.1 (a), Ob.dep.5 (b), Ob.dep.4 sites (c). Bottom is 10 cm beneath the deepest point of concentration measurement



consist of silt leading to low hydraulic conductivity and to prolonged inundation after the flooding. Under these conditions layer rich in organic matter formed in floodplain depressions. The most similar high-latitude floodplains were studied by van Huissteden et al. (2005) in arctic tundra where unusually high fluxes and variability were found. Authors suggested that the latter was caused by higher primary productivity of the floodplain vegetation, and enhanced supply of substrate for methanogens from floodwater. Wang et al. (2006) carried out measurements at freshwater marshes of the Xilin River, Inner Mongolia with similar climatic conditions; they also obtained very high emission rates, especially from organic marshes. However, abovementioned studies stand apart from other researches showing considerably lower CH_4 flux rates.

Water Column Stratification

Surface water methane concentrations as well as the contribution of diffusive flux to the total emission at the Mu.wet.1 and Ob.dep.4 sites are of the same order of magnitude with the ones measured in wetland lakes within the same region (Repo et al. 2007). However, diffusive flux was less pronounced at Ob.dep.5 site. We suggest that strong insolation in the absence of clouds as well as the low wind speed (1.5 m/s at 10 m height) could result in the daytime stratification during the measurements at Ob.dep.5 site. Probably, the stratification was not stable and could be destroyed in the nighttime due to the cooling of surface water (Ford et al. 2002). The water depth at the Mu.wet.1 and Ob.dep.4 sites was considerably lower (1 m vs. 2.5 m at Ob.dep.5 site) making stratification not possible (Wetzel 2001). Measurements of dissolved methane concentration confirmed the presence of stratification since the CH_4 concentration was 10 times higher in bottom waters (10 cm above the sediments) at the Ob.dep.5 than at Mu.wet.1

and Ob.dep.4 sites. We also observed higher temperature gradient at Ob.dep.5 site as another indicator of the water column stratification.

Relevant Transport Mechanisms at Hot Moments of Methane Emission

In most cases, obtained methane fluxes varied in the range of units and depended on hydrological conditions and sediment type. Additionally, spatial variations of the methane fluxes were enormous and emissions varied 3 to 4 times despite the fact that they were located at one meter from each other within the pairs Ob.ts.1–2 and Ob.ts.3–4. On the other hand, fluxes frequently changed during the consecutive measurements at the same site that raises questions about the origin of such variability.

Interestingly, similar emission patterns had already been observed in the shallow taiga wetland lakes (Sabrekov et al. 2013) and such variations were attributed to the active ebullition, and the evidence suggested that variability was highest when the measurements were conducted from the portable «bridges». In that study, the usage of boat resulted in less variable and more consistent fluxes (Sabrekov et al. 2013), because they excluded soil disturbance, while bridges created a risk of artificial bubbling. We suggest the same effect to be observed at Ob.ts.1–4 sites where only portable «bridges» were used in comparison to measurements from the boat at Ob.dep.4–5 and Ob.el.wet.2 sites. Our observations showed that many bubbles were emitted during the chamber installation process. Panikov's test² also provided additional supportive results for the presence of bubbles in the study sites. Unfortunately, soil disturbance during the

² forced disturbance of wetland surface to reveal the presence of bubbles in the sediments

Table 3 Studies on methane fluxes from floodplains

Site	Methane flux, $\text{mgC}\cdot\text{m}^{-2}\cdot\text{h}^{-1}$	Reference
Arctic tundra soils on a river floodplain	Wet backswamp sites	Mean: 13.5 ± 10.5
	Dry sites	Mean: 0.78 ± 1.28
Forested floodplain of the Ogeechee River, USA	East floodplain, low habitat	–0.6 – 18.2 Mean: 2.6
	West floodplain, low habitat	–0.6 – 10.3 Mean: 0.8
Creeping Swamp, North Carolina, USA	0–10; Mean: 3	Mulholland 1981
Sabine River Floodplain, USA	0 to 68.3	Bianchi et al. 1996
Orinoco River, Venezuela	Flooded forest / Macrophytes Open water	Median: 0.72 Median: 0.26
The Mary River, northern Australia	0 to 115; Mean: 19	Bass et al. 2014
Australian Floodplain Wetland	Eleocharis beds	<0.12 to 33
	Myriophyllum beds	<0.12 to 11.3
	Open water with Vallisneria	<0.12 to 19.7
	Ebullition	0.6 to 19.3
Amazonian floodplain wetlands	Open water	2.31 ± 0.44
	Grass mat	6.28 ± 1.09
	Flooded forest	3.94 ± 0.63
Created riparian wetland, Schiermeier Olentangy River, USA	With macrophytes, dry	1.32 ± 0.26
	With macrophytes, wet	4.70 ± 0.54
	Without macrophytes, dry	2.10 ± 0.92
	Without macrophytes, wet	3.93 ± 1.10
Freshwater marshes of the Xilin River, inner Mongolia	Organic marsh, «the patch»	28.4 to 42.5
	Organic marsh, «the vicinity»	4.6 to 14
	Sandy marsh, «the patch»	7.8 to 10.4
	Sandy marsh, «the vicinity»	1.8 to 3.4
Freshwater created riverine marshes, central Ohio, USA	Plant self-colonized wetland	3.6
	Planted wetland	3.3

measurements limited the study, since the water table level was too low to use a boat. However, measurements from «bridges» at Ob.dep.1–3 sites, showing much lower fluxes rates, suggest that besides «bridges» other factors may also play a role here.

Apparently, soil disturbance may be the factor for high fluxes and their variability only when sediments contain large amount of methane trapped as gas bubbles. We hypothesize that gas bubbles were accumulated during the inundated period when the gas diffusion rate was limited due to the high water saturation of sediments with high silt and mineral contents. In addition, low methane solubility (2 orders of magnitudes smaller than CO_2 solubility) and high hydrostatic pressure also contributed to bubble formation and accumulation. Actually, measurements of dissolved methane concentration in sediments at nearby sites in June 2016 revealed more than 10 times higher CH_4 concentration compared to it in the water column. Observed heterogeneity of fluxes could be corresponded to different ebullition rates due to the local differences of geochemical conditions, bulk density, vegetation cover, organic content, etc.

Another interesting CH_4 flux pattern was related to the temporal dynamic at Ob.ts.2–4 sites where unusual high fluxes had been observed during ten days after main water drawdown (13–17 August) with further gradual decreasing of emissions and their dispersion (Fig. 3). We suggested that methane release was triggered by abrupt hydrostatic pressure decrease induced by water drawdown. It has been shown that CH_4 flux changes by 2 orders of magnitudes within a matter of tens of seconds owing to the release of free-phase CH_4 (Tokida et al. 2007). The evidence suggested that the threshold concentration of dissolved methane correlate with the water column depth (Stepanenko et al. 2011); its drop might lead to gas generation from solution and the enlargement of the volume of the gas phase with further ebullition. Similar observations were found in the literature: variations in hydrostatic pressure controlled by diurnal tides triggered ebullition from subtidal freshwater sediments dominated by methanogenesis in the White Oak River estuary, North Carolina (Chanton et al. 1989) where pulses of gas consisting of 50–80% methane were released when the tidal cycle reached its minimum. In Amazon River floodplain, the frequency of bubbling and its

contribution to total flux was lower during the period of rising water table compared to the falling period (Bartlett et al. 1990). Moore et al. (1990) described that lowering the water table in fens of subarctic Quebec by 5–10 cm led to degassing of CH₄ emission rates. Bubbling was most intense during water table drop and bubbling diminished as the water level of the Gatun Lake rose (Keller and Stallard 1994). Several studies in tidal systems have shown that bubbling occurred in discrete episodes as hydrostatic pressure was released during low tide (Martens 1976; Martens and Klump 1980; Chanton et al. 1989). At Cape Lookout Bight, a total pressure change of approximately 0.03 atm corresponding to a tidal depth of 0.3 m was sufficient to produce bubbling (Martens and Klump 1980) (Keller and Stallard 1994). Fechner-Levy and Hemond (1996) showed that changes in atmospheric pressure, temperature, and water-table elevation might result in modulation of the ebullitive CH₄ flux. Recently, Chamberlain et al. (2016) found that methane emissions lag water table fluctuations, and peak fluxes occur during water table recession. Thus, evidence suggests that changes in absolute hydrostatic pressure clearly affect the amount of ebullition that occurs sediments and, thus, total methane flux and its variability.

Challenges and Prospects

The ebullitive CH₄ flux from the soil surface is difficult to quantify due to its episodic nature. In the ideal scenario, the methane fluxes in such heterogeneous environment should be measured by micrometeorological methods at short temporal scales (in order to capture scattered ebullition events). To our knowledge, there were no such measurements in Ob' floodplain and only now experimental techniques are being developed for peat soils to systematically analyze the effects of external hydrostatic pressure and temperature on frequency of bubble formation and ebullition thresholds (Ramirez et al. 2016). Measurements by floating chamber may give reliable results in case of using a boat; the latter prevent additional disturbing of soil that may release gas bubbles, artificially. Standard bubble traps are hardly applicable after water subsiding; however, they may provide interesting data about ebullition rates during the flooding period. Future investigations should include the role of air pressure drop that is a process similar to hydrostatic pressure drop. Overall, systematic measurements at high sensitivity are needed to capture the short term and local scale variations of the environmental conditions (e.g., water table, temperature) in their effects on methane fluxes.

Acknowledgments The reported study was supported by RFBR, research project No. 15-05-07622 a.

References

- Altor AE, Mitsch WJ (2006) Methane flux from created riparian marshes: relationship to intermittent versus continuous inundation and emergent macrophytes. *Ecological Engineering* 28: 224–234
- Bartlett KB, Harriss RC (1993) Review and assessment of methane emissions from wetlands. *Chemosphere* 26:261–320
- Bartlett KB, Crill PM, Bonassi JA, Richey JE, Harriss RC (1990) Methane flux from the Amazon River floodplain: emissions during rising water. *Journal of Geophysical Research: Atmospheres* 95: 16773–16788
- Bass A, O'Grady D, Leblanc M, Tweed S, Nelson P, Bird M (2014) Carbon dioxide and methane emissions from a wet-dry tropical floodplain in northern Australia. *Wetlands* 34:619–627
- Bianchi T, Freer M, Wetzel R (1996) Temporal and spatial variability, and the role of dissolved organic carbon (DOC) in methane fluxes from the Sabine River floodplain (Southeast Texas, USA). *Archiv für Hydrobiologie* 136:261–287
- Bohn TJ, Melton JR, Ito A, Kleinen T, Spahni R, Stocker BD, Zhang et al (2015) WETCHIMP-WSL: intercomparison of wetland methane emissions models over West Siberia. *Biogeosciences* 12:3321–3349. <https://doi.org/10.5194/bg-12-3321-2015>
- Boon PI, Sorrell BK (1995) Methane fluxes from an Australian floodplain wetland: the importance of emergent macrophytes. *Journal of the North American Benthological Society* 14:582–598
- Chamberlain SD, Gomez-Casanovas N, Walter MT, Boughton EH, Bernacchi CJ, DeLucia EH, Groffman PM, Keel EW, Sparks JP (2016) Influence of transient flooding on methane fluxes from subtropical pastures. *Journal of Geophysical Research: Biogeosciences* 121:965–977
- Chanton JP, Martens CS, Kelley CA (1989) Gas transport from methane-saturated, tidal freshwater and wetland sediments. *Limnology and Oceanography* 34:807–819
- Cole JJ, Prairie YT, Caraco NF et al (2007) Plumbing the global carbon cycle: integrating inland waters into the terrestrial carbon budget. *Ecosystems* 10:172–185. <https://doi.org/10.1007/s10021-006-9013-8>
- Fechner-Levy EJ, Hemond HF (1996) Trapped methane volume and potential effects on methane ebullition in a northern peatland. *Oceanography* 41:1375–1383
- Ford PW, Boon PI, Lee K (2002) Methane and oxygen dynamics in a shallow floodplain lake: the significance of periodic stratification. *Hydrobiologia* 485:97–110
- Glagolev M, Kleptsova I, Filippov I, Maksyutov S, Machida T (2011) Regional methane emission from West Siberia mire landscapes. *Environmental Research Letters* 6:045214. <https://doi.org/10.1088/1748-9326/6/4/045214>
- Kahaner D, Moler C, Nash S (1989) Numerical methods and software. Englewood Cliffs: Prentice Hall, 1989 1:
- Keller M, Stallard RF (1994) Methane emission by bubbling from Gatun Lake, Panama. *Journal of Geophysical Research: Atmospheres* 99: 8307–8319
- Kim HS, Maksyutov S, Glagolev MV, Machida T, Patra PK, Sudo K, Inoue G (2011) Evaluation of methane emissions from west Siberian wetlands based on inverse modeling. *Environmental Research Letters* 6:035201. <https://doi.org/10.1088/1748-9326/6/3/035201>
- Krasnov OA, Maksyutov SS, Davydov DK, Fofonov AV, Glagolev MV (2015) Measurements of methane and carbon dioxide fluxes on the Bakchar bog in warm season. 21st International Symposium Atmospheric and Ocean Optics: Atmospheric Physics (November 19, 2015). 968066 <https://doi.org/10.1117/12.2205557>
- Malanson GP (1993) Riparian landscapes. Cambridge University Press Publ

- Martens CS (1976) Control of methane sediment-water bubble transport by macroinfaunal irrigation in Cape Lookout bight, North Carolina. *Science* 192:998–1000
- Martens CS, Klump JV (1980) Biogeochemical cycling in an organic-rich coastal marine basin-I. Methane sediment-water exchange processes. *Geochimica et Cosmochimica Acta* 44:471–490
- Melack JM, Hess LL, Gastil M, Forsberg BR, Hamilton SK, Lima IB, Novo EM (2004) Regionalization of methane emissions in the Amazon Basin with microwave remote sensing. *Global Change Biology* 10:530–544
- Moore T, Roulet N, Knowles R (1990) Spatial and temporal variations of methane flux from subarctic/northern boreal fens. *Global Biogeochemical Cycles* 4:29–46
- Mulholland PJ (1981) Organic carbon flow in a swamp-stream ecosystem. *Ecological Monographs* 51:307–322
- Nahlik AM, Mitsch WJ (2010) Methane emissions from created riverine wetlands. *Wetlands* 30:783–793
- Postnov A, Stulov E, Strunin M, Khattatov V, Tolchinsky Y, Inoue G, Tohjima Y, Maksyutov S, Machida M (1994) Vertical turbulent transport of methane in the atmospheric boundary layer over the Central Western Siberia—airborne measurements of greenhouse gases over Siberia VI. Proceedings of the international symposium on global cycles of atmospheric greenhouse gases (march 7-10, 1994, Sendai, Japan).—Sendai 30-33
- Pulliam WM (1993) Carbon dioxide and methane exports from a southeastern floodplain swamp. *Ecological Monographs* 63:29–53
- Ramirez JA, Baird AJ, Coulthard TJ (2016) The effect of pore structure on ebullition from peat. *Journal of Geophysical Research: Biogeosciences* 121:1646–1656. <https://doi.org/10.1002/2015JG003289>
- Rasilo T, Prairie YT, Giorgio PA (2015) Large-scale patterns in summer diffusive CH₄ fluxes across boreal lakes, and contribution to diffusive C emissions. *Global Change Biology* 21:1124–1139
- Repo M, Huttunen J, Naumov A, Chichulin A, Lapshina E, Bleuten W, Martikainen P (2007) Release of CO₂ and CH₄ from small wetland lakes in western Siberia. *Tellus B* 59:788–796
- Ringeval B, Houweling S, van Bodegom PM, Spahni R, van Beek R, Joos F, Röckmann T (2014) Methane emissions from floodplains in the Amazon Basin: challenges in developing a process-based model for global applications. *Biogeosciences* 11:1519–1558. <https://doi.org/10.5194/bg-11-1519-2014>
- Sabrekov AF, Kleptsova IE, Glagolev MV, Maksyutov SS, Machida T (2011) Methane emission from middle taiga oligotrophic hollows of Western Siberia. *TSPU Bulletin* 5:135–143
- Sabrekov A, Glagolev M, Kleptsova I, Machida T, Maksyutov S (2013) Methane emission from mires of the west Siberian taiga. *Eurasian Soil Science* 46:1182–1193
- Sabrekov AF, Runkle BRK, Glagolev MV, Kleptsova IE, Maksyutov SS (2014) Seasonal variability as a source of uncertainty in the west Siberian regional CH₄ flux upscaling. *Environmental Research Letters* 9:045008. <https://doi.org/10.1088/1748-9326/9/4/045008>
- Schütz H, Holzapfel-Pschorn A, Conrad R, Rennenberg H, Seiler W (1989) A 3-year continuous record on the influence of daytime, season, and fertilizer treatment on methane emission rates from an Italian rice paddy. *Journal of Geophysical Research: Atmospheres* 94:16405–16416
- Segers R (1998) Methane production and methane consumption: a review of processes underlying wetland methane fluxes. *Biogeochemistry* 41:23–51
- Sharkey TD, Holland EA, Mooney HA (1991) Trace gas emissions by plants. San Diego, CA (United States); Academic Press, Inc.
- Smith LK, Lewis WM Jr, Chanton JP, Cronin G, Hamilton SK (2000) Methane emissions from the Orinoco River floodplain, Venezuela. *Biogeochemistry* 51:113–140
- Stepanenko V, Martynov A, Joehnk KD, Perroud M, Fang X, Subin ZM, Beyrich F, Nordbo A, Mironov D, Huotari J (2011) Thermal regime and water–atmosphere interactions of shallow mid-latitude lakes: a case study within the framework of the Lake Model Intercomparison Project
- Stocker T et al (2013) IPCC, 2013: the physical science basis. Contribution of working group I to the fifth assessment report of the intergovernmental panel on climate change
- Tokida T, Miyazaki T, Mizoguchi M, Nagata O, Takakai F, Kagemoto A, Hatano R (2007) Falling atmospheric pressure as a trigger for methane ebullition from peatland. *Global Biogeochemical Cycles* 21. <https://doi.org/10.1029/2006gb002790>
- van Huissteden J, Maximov TC, Dolman AJ (2005) High methane flux from an arctic floodplain (Indigirka lowlands, eastern Siberia). *Journal of Geophysical Research: Biogeosciences* 110. <https://doi.org/10.1029/2005jg000010>
- Wang Z, Han X, Li L (2006) Methane emission patches in riparian marshes of the inner Mongolia. *Atmospheric Environment* 40: 5528–5532. <https://doi.org/10.1016/j.atmosenv.2006.04.045>
- Wetzel RG (2001) Lake and river ecosystems. Limnology, Academic Press, London 1006
- Whalen SC (2005) Biogeochemistry of methane exchange between natural wetlands and the atmosphere. *Environmental Engineering Science* 22:73–94